Scholars Journal of Engineering and Technology

OPEN ACCESS

Abbreviated Key Title: Sch J Eng Tech
ISSN 2347-9523 (Print) | ISSN 2321-435X (Online)
Journal homepage: https://saspublishers.com

Flood Forecasting in Vientiane Capital, Laos based on the Analytic Hierarchy Process (AHP) Method in Remote Sensing

Phonekham Hansana[1*]

[1]College of Electrical and Information Engineering, Hunan University, Changsha 410082, China

DOI: 10.36347/sjet.2024.v12i08.001 | **Received:** 21.06.2024 | **Accepted:** 29.07.2024 | **Published:** 01.08.2024

***Corresponding author:** Phonekham Hansana
College of Electrical and Information Engineering, Hunan University, Changsha 410082, China

Abstract | **Original Research Article**

Introduces a flood risk prediction algorithm based on the Analytic Hierarchy Process (AHP), a robust decision-making methodology known for its simplicity and effectiveness in systematically evaluating and prioritizing multiple criteria. Utilizing the Analytic Hierarchy Process (AHP) entails the development of a hierarchical framework encompassing standards and options. It involves assigning numerical values to individual criteria and employing Comparisons conducted in pairs to ascertain their concerning other factors or comparison to a reference point significance. In the specific context of flood risk prediction, four crucial factors within the Analytic Hierarchy Process are considered: rainfall patterns, vertical elevation, proximity to the river, and Land Use/Land Cover (LULC). These factors, closely linked to floods, are essential considerations in flood risk analysis. After conducting a comprehensive analysis of different elements, the proposed method categorizes flood risk into five levels: the smallest level, small level, middle level, high level, and highest level. The flood risk prediction algorithm begins by constructing a pairwise comparison matrix to quantify the significance of each variable concerning flooding occurrences. Subsequently, leveraging this matrix along with data on rainfall patterns, vertical elevation, river distance, and the utilization and composition of land (Land Use/Land Cover - LULC), The algorithm computes and evaluates the level of risk associated with flooding. This methodical approach improves the precision and reliability of flood risk predictions, offering valuable insights for developing proactive flood risk management strategies.

Keywords: Flood Forecasting, Remote Sensing, AHP, GIS.

I. INTRODUCTION

The Model-Based Flood Forecasting Method provides a predictive approach using mathematical models to predict the likelihood and severity of floods in a specific area. This approach involves developing and applying hydraulic hydrological and meteorological models to replicate water movements across a river basin, facilitating forecasting of potential inundation. Utilizing the model-based flood prediction approach follows a systematic process that involves collecting thorough data concerning the river basin, such as topography, soil composition, land utilization, and hydrological circumstances. Integrating the Analytical Hierarchy Process (AHP) within the Model-Based Flood Forecasting Method enhances its effectiveness in predicting floods by offering a systematic and comprehensive framework for decision-making. This approach integrates expert insight and adjusts to changing circumstances, enabling more informed decision-making, enhancing capabilities for emergency response, and reducing societal and environmental effects linked to flooding. This model-based flood forecasting method provides precise and timely insights into potential flooding, enabling authorities to implement appropriate measures to mitigate its impact. Additionally, it is invaluable for planning and emergency preparedness, as it identifies high-risk flood zones and helps prioritize mitigation strategies. In summary, the model-based flood forecasting method is a highly effective tool for predicting and managing floods. It delivers early warnings and facilitates preparations that significantly reduce damage and loss of life. The Analytical Hierarchy Process (AHP) technique effectively identified the elements influencing flood risk, enhancing the understanding of the mechanisms driving flood vulnerability. The method of evaluating multi-criteria indices is widely utilized in assessing flood risk assessment [1]. Within this methodology, assigning weights to indices is a crucial aspect [2]. Several techniques, such as the Analytic Hierarchy Process (AHP) [3], fuzzy reasoning [4], and Principal Component Analysis (PCA) [5], are commonly used to

establish the importance coefficients for these indicators. The Analytic Hierarchy Process (AHP) is widely used for its computational simplicity, although it does involve a notable level of subjectivity influenced by the expertise and experience of the experts. Researchers have made efforts to mitigate this subjective nature. Gigovic et al [6] applied two improved AHP techniques, namely, interval approximate value (IR-AHP) and vagueness (F-AHP) are used in evaluating flood risk. The IR-AHP method produced results with the greatest consistency with historical data. In another instance, Lyu and colleagues [7] utilized both the Analytic Hierarchy Process (AHP) technique and the Interval Analytic Hierarchy Process (I-AHP) method to assess the potential flooding in Guangzhou's metro system. The findings indicated that the Interval Analytic Hierarchy Process (I-AHP) approach identified a broader high-risk area. In a separate study, Cai and colleagues [8] Selected 11 criteria for evaluating flood risk in mountainous urban areas, determining the weights assigned to indices through the AHP method using triangular fuzzy numbers (TFN-AHP). The results showed that the approach using triangular fuzzy numbers (TFN-AHP) surpassed traditional AHP in effectively assessing flood risk in mountainous urban areas.

Urban flooding is a significant and recurring natural disaster in cities. Rapid urbanization has concentrated populations and economic activities in urban areas, amplifying the social and economic damage caused by floods to pre-urbanization times. Mitigating the negative impacts of urban flooding has become a top priority in urban disaster management strategies. An effective approach to addressing this concern is urban flood risk assessment, which is a valuable tool for identifying risk levels and the primary factors contributing to flooding in various areas. This assessment forms the foundation for developing strategies to prevent and mitigate urban flooding floods. In an era marked by significant advancements in earth observation technology and computational capabilities, there is a growing emphasis on large-scale flood mapping and flood risk assessment. Integrating machine learning methods into these processes is becoming increasingly prevalent, leveraging rapid advancements in earth observation and computing technology capabilities.

The AHP method, enhanced with D-numbers, is commonly referred to as D-AHP. This approach has been successfully applied in various contexts, including vendor selection [9] and the evaluation of curtain grouting effectiveness [10]. The AHP method enhanced with D-numbers preserves the simplicity of AHP calculations and the clarity of hierarchical logic, while effectively addressing the adverse effects of uncertain and incomplete evaluation information. As a result, the Disaggregation Analytic Hierarchy Process (D-AHP) method was chosen to determine the significance of indices in assessing the risk of urban flooding in this research. Once the criterion weights are established, the next step involves categorizing the level of flood risk. Thoughtful assessment of risk levels is a critical stage in urban flood risk assessment, and clustering algorithms provide a data-driven methodology capable of categorizing data in the absence of explicit categorization standards. Xu and colleagues [12] utilized the k-means clustering technique to evaluate flood vulnerability classification in Haikou City, China, achieving satisfactory results. However, constraints of the k-means algorithm were identified [11]. Importantly, the number of clusters must be predetermined, which can be challenging in the initial stages of grouping. Furthermore, since the starting cluster center is chosen randomly, the outcome of each iteration is heavily influenced by this initial selection.

However, the methodologies mentioned earlier assumed complete evaluation information. In practice, expert evaluations within the Analytic Hierarchy Process (AHP) inherently introduce uncertainties such as imprecision, vagueness, and incompleteness, stemming from subjective judgments made by individuals. For example, during the pairwise comparison of index importance, two typical scenarios can occur: (i) lack of consensus among experts resulting in divergent evaluations, and (ii) cases where some experts may refrain from providing evaluations due to differences in their respective research domains. In such situations, traditional AHP methods may prove impractical or produce unsatisfactory evaluation results. To tackle the challenge of uncertain information, Deng et al. introduced the theory of D-numbers, which extends the Dempster-Shafer evidence theory—a framework widely employed in information fusion systems. The theory of D-numbers successfully overcomes the constraints of the Dempster-Shafer evidence theory in handling ambiguous data. Unlike the Dempster-Shafer theory, it does not necessitate the fulfillment of the completeness constraint for the basic probability assignment (BPA) and can effectively manage incomplete data. Therefore, the fuzzy preference relationship extended by D-numbers serves as a representation of the decision matrix resulting from pairwise comparisons made by AHP experts, providing a solution to challenges arising from uncertain evaluation information [13].

This section is dedicated to generating a map indicating areas prone to flooding utilizing the Analytic Hierarchy Process (AHP) and Geographic Information System (GIS) software. The Analytic Hierarchy Process (AHP) is a straightforward yet powerful decision-making process approach enabling decision-makers to systematically and objectively prioritize and assess various criteria. In the context of AHP, four factors rainfall pattern, elevation, proximity to the river, and Land Use and Land Cover (LULC) were considered. These elements were reclassified into five risk categories, comprising the spectrum of risk including

gradations such as minimal, low, moderate, high, and maximal risk.

1) The precipitation arrangement serves as a pivotal cause associated with inundation, amplifying the volume of hydrological flow within riverine and stream environments, leading to an inundation of the magnitude, duration, and spatial dispersion of precipitation occurrences impacting the nearby regions are critical factors influencing the magnitude and scope of inundation.
2) Elevation, synonymous with altitude relative to sea level, is a crucial determinant of flood vulnerability. Low-lying areas are more susceptible to inundation as they are prone to water accumulation. The elevation of a location significantly influences its vulnerability to inundation.
3) Proximity to the river is a decisive factor influencing flood susceptibility in a specified region. Regions situated proximate to a river face a heightened likelihood of flooding, since water may inundate from the river channel during periods of elevated flow. Conversely, locations situated at a greater distance from a river typically exhibit a diminished risk of flooding owing to a decreased probability of river overflow impacting them.
4) Land Use and Land Cover (LULC) plays a pivotal influence in shaping the frequency and severity of flood occurrences. Regions accompanied by significant amounts of impermeable surfaces, like those found in urban environments areas, face an increased likelihood of inundation because of heightened surface runoff during periods of intense precipitation. In contrast, areas with indigenous vegetation or porous surfaces, like woodlands or prairies, exhibit a decreased risk of flooding as they have the capacity to absorb and retain water. Alterations or changes in Land Use and Land Cover (LULC), including activities such as deforestation, urbanization, or agricultural expansion, may modify related to water systems phenomena within a locality, exacerbating the likelihood of inundation.

Additionally, the regularity ratio The coherence (CR) of weights, as expressed in Equation (4-2) provided below, served to assess and ascertain the scientific validity of the comparison matrix.

In Equation (4-1), λ_{max} λ max denotes the highest eigenvalue associated with the comparison matrix, and n represents the arrangement pertaining to the comparison matrix, which equals 4 in this study. In Equation (4-2), RI signifies the random nature consistency indicator, with its value determined according to the arrangement of the comparison matrix; for this work, RI is 0.8931. The computed Consistency Ratio of 0.1, derived as per the equation (4-2) suggests indicating that the matrix for pairwise comparisons employed in this research is deemed plausible and scientifically sound.

Subsequently, the weights for each factor in the Analytic Hierarchy Process (AHP) were calculated using Equation (4-3). In Equation (4-3), the variable n remains consistent with its definition in Equation (4-1) and also w denotes the weight assigned to every single component. The variables i, j, k represent the i_{th}, j_{th}, k_{th} values, ranging from 1 to n. Consequently, the importance coefficients attributed regarding absolute rainfall patterns elevation, Distance from the river, as well as Land Use and Land Cover (LULC) were determined as 0.62, 0.05, 0.09, and 0.25, correspondingly.

Finally, AHP was employed to produce the ultimate flood risk map utilizing the prescribed formula and corresponding weights: where R_a, H, R_i, L represented the rainfall pattern, absolute height, distance from the river, and land use and land cover (LULC) characteristics, in sequence. The resultant flood risk map generated through AHP analysis was stratified into five distinct risk levels, from minimal to maximal risk. For a comprehensive understanding of the correlation between the flood monitoring results and the flood risk map, In this investigation, Pearson correlation coefficients and associated P-values were employed to validate their relationship. Pearson correlation coefficients may be depicted. In Equation (4-5), X_i, Y_i are the i-point observations corresponding to variables X, Y, and $\bar{X}, \bar{Y}$ are these represent the averages of X, Y samples, respectively. r is the correlation coefficient and n is the overall sample count. Besides, The P-values can be computed using the above equation (4-6). CDF represents the cumulative distribution function. t refers to the t-statistic, which can be specified. Where r, n are the correlation coefficient derived from Equation (4-5) and the total number of samples, respectively. Specifically, the correlation coefficient quantifies the extent of the linear relationship between the two variables, with values ranging between -1 and 1. A value of 1 denotes a perfect positive linear correlation, Meanwhile, a value of -1 signifies a perfect negative linear correlation. The P-value quantifies the likelihood of observing a correlation coefficient as extreme as the one obtained by chance, assuming the absence of a genuine correlation between the two variables. A P-value below a certain threshold (e.g., 0.05) indicates statistical significance of the correlation, implying that its occurrence is improbable by chance.

II. RELATED WORKS

2. 1. AHP Flood Risk in Remote Sensing

Flood mapping is essential for decision-making processes related to such events, as it aids in risk management, near real-time forecasting, and the management of land use and land cover (LU/LC). The

complexity of floods as multi-dimensional dynamic phenomena has prompted the widespread use of geographic information system (GIS) and remote sensing (RS) data to delineate the extent of flooded areas. Ensuring near-real-time flood monitoring is vital for effective mitigation and control of their impact [14]. Research conducted by Sofia et al [15], emphasizes the importance of cumulative flood hazard delineation, considering environmental degradation and climate change factors associated with LU/LC changes, to enhance monitoring capabilities. However, pixel-based flood analysis requires significant time and processing power to achieve near-real-time assessment. Flood vulnerability assessment combines inundation extent with social data to identify communities most at risk for property damage and loss of life. In developed countries with high population density, flood exposure, and vulnerability are currently mapped using hydrodynamic inundation models combined with high-resolution population distribution data. Different models, such as the adaptive neuro-fuzzy inference system for landslide susceptibility in Qazvin Province, Iran [16], hydraulic modeling to estimate unsaturated soil hydraulic conductivity [17], and the Soil and Water Assessment Tool (SWAT) integrated into ArcGIS software environment [18], are used for flood susceptibility estimation. Deep learning methods such as artificial neural networks (ANNs), fuzzy logic, support vector machines (SVM), random forest classification, regression trees (RTs), and classification and regression trees (CART) algorithms [19], have considerable potential for accurate flood mapping and monitoring. Although artificial neural networks (ANNs) are extensively utilized for flood susceptibility mapping, they have been noted for drawbacks such as over-fitting, under-fitting, slow learning, the curse of dimensionality, and slow convergence to a local optimum. Moreover, its capability to handle complex hydrological phenomena has been found inadequate. Tellman et al [20] introduced an innovative approach to flood modeling, utilizing satellite imagery within a cloud computing-enabled Google Earth Engine (GEE) system. This methodology enables real-time mapping of flood hazards through the generation of a globally consistent flood inundation layer and the dynamic modeling of flood-susceptible areas. A cloud computing GEE-based Flood Prevention and Emergency Response System (FPERS) was successfully developed and implemented for three key scenarios: pre-flood, post-flood, and during flood events caused by typhoons or torrential rain in China from 2013 to 2016 [21]. For creating a specialized decision-making framework in flood susceptibility mapping, the analytical hierarchy process (AHP) emerges as the preferred technique [22]. Within the AHP, various flood vulnerability parameters are systematically ranked based on their impact, employing Pairwise Comparison Matrices (PCMs) [23]. This selected methodological framework captures the cumulative nature of each criterion, proving effective in generating flood data across spatial scales, including local, regional, and national levels. Bihar, characterized by numerous rivers, is identified as a flood-prone region, constituting 16.5 percent of the total flood area and housing 22.1 percent of the flood-affected population in India [24].

2.2. The cloud computing-enabled Google Earth Engine (GEE) system

Google Earth Engine (GEE) is a cloud-based computing platform that leverages Google's infrastructure to facilitate the retrieval and processing of geospatial data [25]. Access to this platform requires an account, and it is provided free of charge for educational and research purposes. The overarching goals of GEE include: (i) creating a dynamic platform for developing algorithms at a large scale; (ii) promoting high-impact research through free and open access; and (iii) contributing to global initiatives addressing the demand and management of big data [26]. GEE features a vast petabyte-scale catalog that consolidates data from diverse sources such as Landsat, Sentinel, and MODIS satellites, along with information on climate models, temperature, and geophysical data characteristics [27]. Its user-friendly interface includes a code editor (available at https://code.earthengine.google.com/, last accessed on January 30, 2023), functioning as an integrated development environment (IDE) for algorithm development using the JavaScript programming language [28]. The platform also supports Python, facilitated through the Earth Engine library [29]. Furthermore, it includes a streamlined interface called "Explorer" (accessible at https://explorer.earthengine.google.com/ workspace, last accessed on January 30, 2023), tailored for users who have limited programming experience. Both interfaces facilitate importing local data and exporting information for further processing or visualization within geographic information systems (GIS) software, such as QGIS (Version 3.28) and ArcGIS Pro (Version 3.1.2), among others.

Research methodologies continually evolve and innovate to construct knowledge [30]. Within the realm of geoscience and remote sensing, Google Earth Engine (GEE) has emerged as a potent tool for remote sensing, finding diverse applications across domains such as agricultural productivity, vegetation monitoring, grassland monitoring, mangrove mapping, land use, and cover, risk and disaster management, islands of heat, surface temperature [31]. The myriad applications underscore the GEE platform’s capacity to handle extensive datasets, thereby contributing significantly to the advancement of scientific research [32]. Numerous researchers have scrutinized the diverse applications of GEE in recent years. Kumar and Mutanga conducted an analysis of literature published between 2011 and 2017 to elucidate the platform’s uses, trends, and potential since its inception. In a different vein, Tamiminia et al undertook a systematic review of GEE in geographic big data applications. Bibliometric analysis, employed in these studies, serves to identify gaps and research

directions within a specific area. Furthermore, it yields objective results that enhance our understanding of the impact and influence of the knowledge area, discerning the evolution of publications. The methodology involves processing bibliographic information, constructing structural maps of the fields, and conducting quantitative analyses of existing academic literature. In recent years, there has been a notable surge in the number of publications utilizing Google Earth Engine (GEE). In light of this trend and recognizing its significance, this research is dedicated to generating knowledge through a bibliometric approach, specifically employing GEE as a focal point. The aim is to derive a quantitative and comprehensive assessment of the topic by conducting citation, co-citation, and co-occurrence analyses. Moreover, the research endeavors to assist researchers in comprehending the progress within this domain, pinpointing proposed works, and fostering innovation in future applications.

2.3. The Rainfall, DEM, Stream, and LULC

Several well-documented methodologies for evaluating flood risk include the application of physical process-based models, notably hydrological models like WATFLOOD. These methods include techniques such as continuous simulation using rainfall-runoff models [33], and statistical methods, such as fitting a probability distribution function to a dataset of annual maximum values (as illustrated in). While both physical-based (mechanistic) and statistical models have proven robust in flood modeling, their effectiveness relies on the availability of streamflow observations for model calibration and validation. However, challenges arise when observational records are either completely unavailable, accessible for only a limited timeframe, or contain data gaps, thus limiting their full potential for flood risk assessment modeling [34]. To overcome these challenges, the integration of advanced geospatial technologies like Geographic Information Systems (GIS) and remote sensing, combined with the application of machine learning algorithms, has greatly improved flood risk assessment. Prominent examples of these algorithms include maximum entropy (MaxEnt) and random forest (RF) [35], K-nearest neighbor (K-NN), decision tree (DT), fuzzy rule-based systems (FRBS), artificial neural networks (ANN), deep neural networks (DNN), adaptive neuro-fuzzy inference system (ANFIS), and support vector machine (SVM). These technologies are particularly advantageous for assessing flood risk in areas where comprehensive hydraulic and hydrological data are not readily available [36].

III. PROPOSED METHOD

3.1. Flood Risk Map in Vientiane Capital, Laos

This section aims to generate a flood risk map using the AHP and GIS software [37]. AHP is a straightforward yet powerful decision-making methodology that enables decision-makers to systematically and objectively prioritize and evaluate multiple criteria. This method entails creating a hierarchy of criteria and alternatives, assigning numerical values to each criterion, and employing pairwise comparisons to establish the relative importance of each criterion. Four elements, namely rainfall pattern, absolute height, distance from the river, and LULC were considered in AHP and reclassified into five classes: minimal risk, low risk, moderate risk, high risk, and maximal risk. As depicted in the flowchart of Figure 2, the study area is Vientiane Capital, Laos of Figure 1.

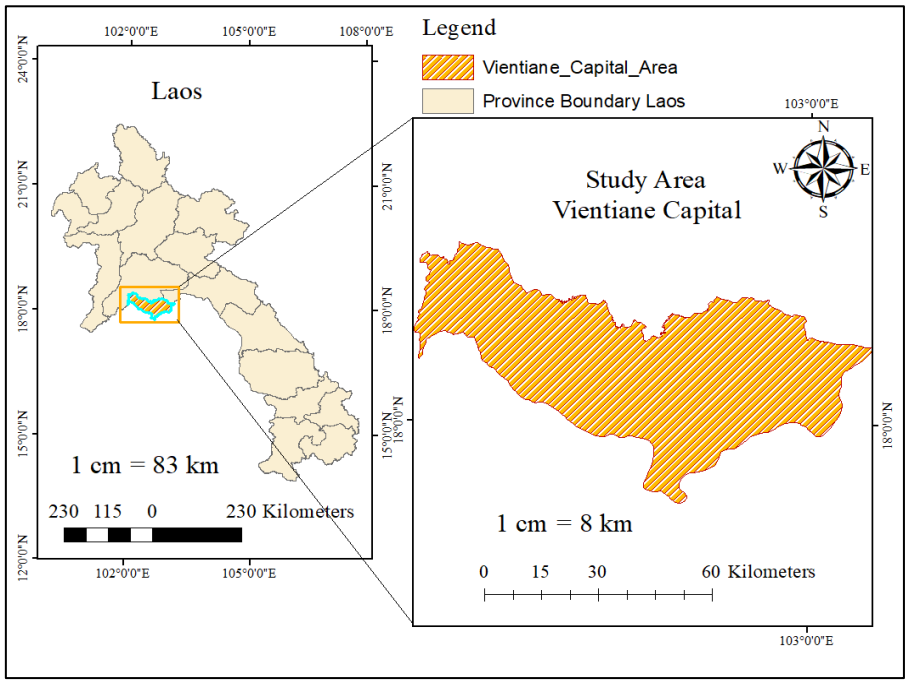

Figure 1: The study area is Vientiane Capital, Laos

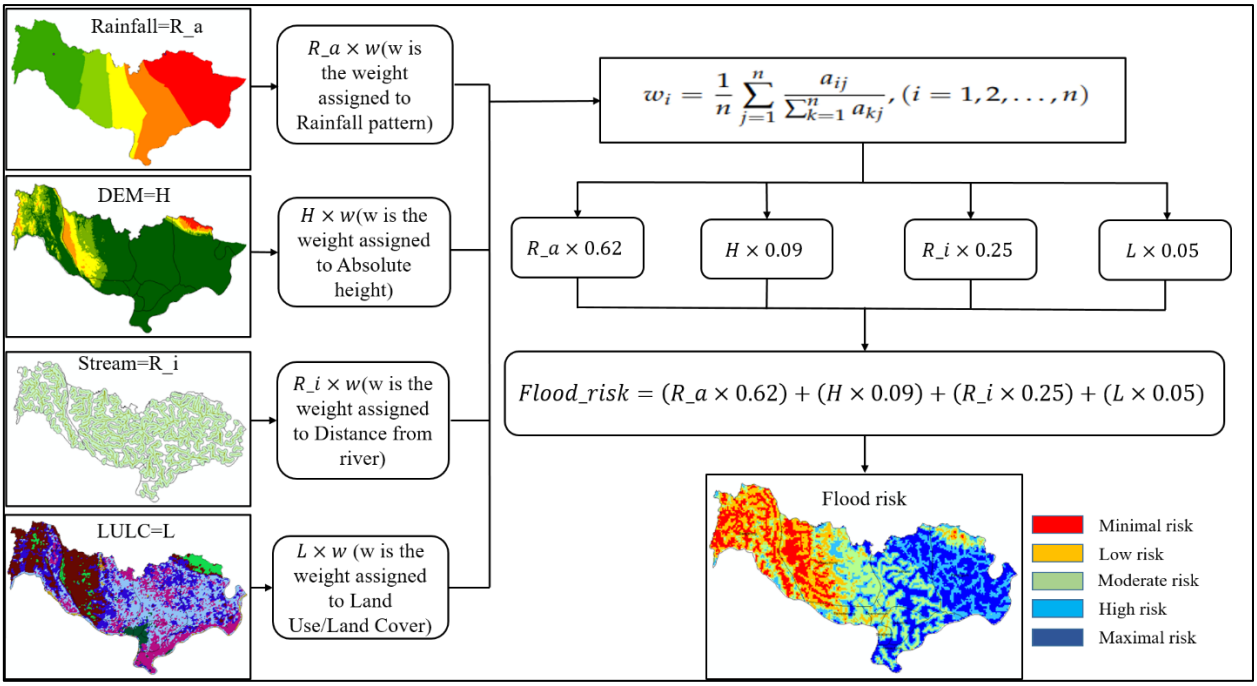

Figure 2: Flow chart of Model-Based Flood Forecasting Method

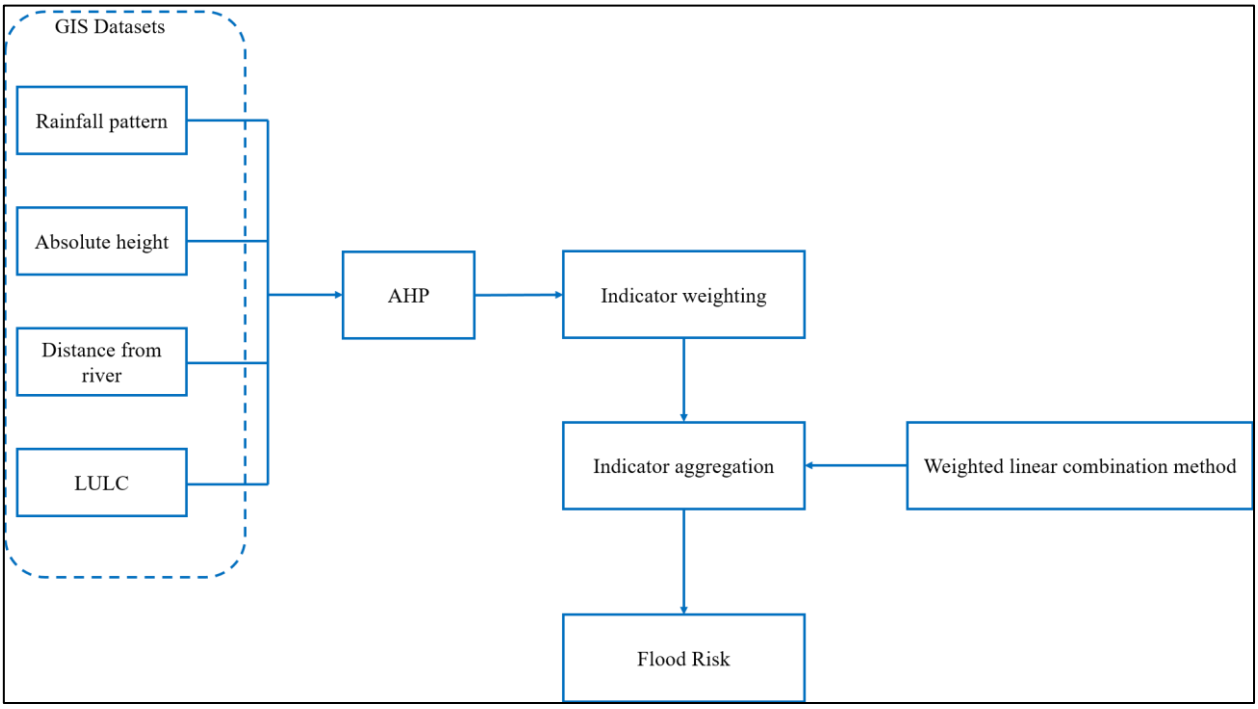

Figure 3: Flow chart of Model-Based Flood Risk Method

1) Rainfall pattern is a crucial factor in flooding, as it raises the water levels in rivers and streams, leading to their banks overflowing and flooding adjacent areas. The intensity, duration, and spatial distribution of rainfall events significantly influence the severity and extent of flooding, as illustrated in Figure 4.

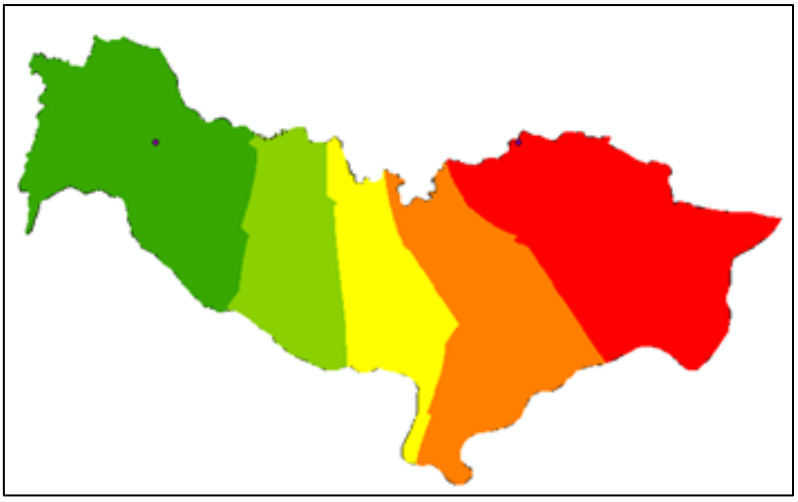

Figure 4: Rainfall in Vientiane Capital, Laos

2) Absolute height, or elevation above sea level, is a critical factor in determining flood risk. Low-lying areas are more susceptible to flooding because water tends to accumulate there, as shown in Figure 5.

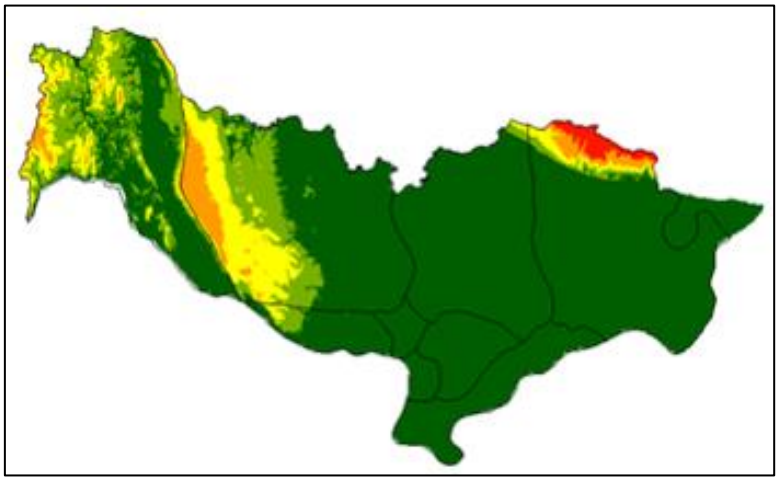

Figure 5: DEM in Vientiane Capital, Laos

3) Distance from the river is a significant determinant of flood risk in a specific region. Areas in close proximity to a river face heightened flood risks, as river channels can overflow during periods of high flow. Conversely, areas situated farther from a river generally experience lower flood risks due to the reduced likelihood of river overflow impacting them. This relationship is illustrated in Figure 6.

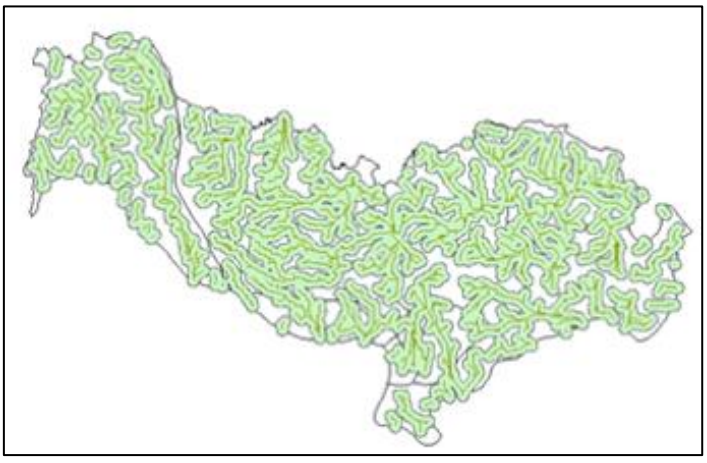

Figure 6: Stream in Vientiane Capital, Laos

4) LULC significantly influence the frequency and severity of flood events. Areas dominated by impervious surfaces, such as urban areas, are more susceptible to flooding due to increased runoff during intense rainfall. Conversely, regions with natural vegetation or permeable surfaces like forests or grasslands experience lower flood risk, as they can absorb and store water. Changes in LULC, such as deforestation, urban development, or agricultural expansion, can modify local hydrological processes and escalate flood risks. This relationship is depicted in Figure 7.

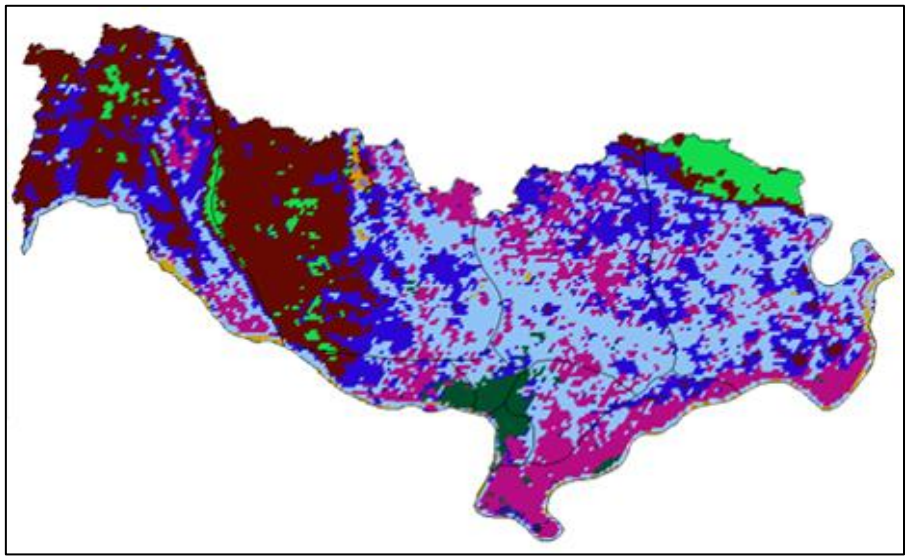

Figure 7: LULC in Vientiane Capital, Laos

The initial stage of AHP involved establishing the pairwise comparison matrix. Based on the importance of each element related to induced flooding as outlined in Table 1, the pairwise comparison matrix for this study is illustrated in Figure 8. Each value in the matrix denotes the relative importance between two factors.

	Rainfall pattern	Absolute height	Distance from river	LULC
Rainfall pattern	1	7	5	9
Absolute height	0.14	1	0.2	3
Distance from river	0.2	5	1	6
LULC	0.11	0.33	0.17	1

9 8 7 6 5 4 3 2 1

Figure 8: Pairwise comparison matrix

Table 1: Pairwise importance

Value	Importance
1	Equally significant
3	Marginally more significant
5	Moderately more significant
7	Considerably more significant
9	Substantially more significant
2,4,6,8	The median value of the aforementioned
Reciprocal	If A/B is 3, then B/A is 1/3

Moreover, the consistency rate (CR) of weights, shown in Equation (4-2) below, could test and determine whether the comparison matrix is scientific.

$$CI = \frac{\lambda_{max} - n}{n-1} \text{ …….. (1)}$$

In Equation (4-1), λ_{max} is the maximum eigenvalue of the comparison matrix, n is the order of the comparison matrix and it is 4 in this work.

$$CR = \frac{CI}{RI} \text{ ……. (2)}$$

In Equation (2), *RI* represents a random consistent index and its value is determined based on the order of the comparison matrix. *RI* is 0.8931 in this work. The calculated CR of 0.1 from Equation (2) indicated that the pairwise comparison matrix used in this study was reasonable.

Then, the weights of each factor in AHP could be calculated by the Equation (3) below:

$$W_i = \frac{1}{n} \sum_{j=1}^{n} \frac{a_{ij}}{\sum_{k=1}^{n} a_{kj}}, \ (i=1, 2..., n) \text{ …… (3)}$$

In Equation (3), *n* is same as Equation (1), and *w* is weight of each element. *i*, *j*, *k* are i_{th}, j_{th}, k_{th} values from 1 to *n*, respectively. As a result, the weights assigned to Rainfall pattern, Absolute height, Distance from river, and LULC were 0.62, 0.09, 0.25, and 0.05, respectively. Finally, AHP was used to generate the final flood risk map with the following formula and weights:

$$Flood\_risk = (R\_a \times 0.62) + (H \times 0.09) + (R\_i \times 0.25) + (L \times 0.05) \text{ ……. (4)}$$

Where *R_a*, *H*, *R_i*, *L* represent rainfall pattern, absolute height, distance from river and LULC, respectively. The resulting flood risk map of AHP was divided into five levels of risk, ranging from minimal to maximal risk.

3.2. Correlation analysis

To comprehend the relationship between the flood monitoring result and flood risk map, this study adopted the Pearson correlation coefficients and P-values to verify their relationship. Pearson correlation coefficients could be represented as followed:

$$r = \frac{\sum_{i=1}^{n}(X_i - \bar{X})(Y_i - \bar{Y})}{\sqrt{\sum_{i=1}^{n}(X_i - \bar{X})^2}\sqrt{\sum_{i=1}^{n}(Y_i - \bar{Y})^2}} \text{ ……. (5)}$$

In Equation (5), X_i, Y_i are the i-point observations corresponding to variables *X*, *Y*, and $\bar{X}$, $\bar{Y}$ are the the average of *X*, *Y* samples, respectively. *r* is correlation coefficient and *n* is the total number of samples.

$$P = 2 \times (1 - CDF(|t|)) \text{ …… (6)}$$

Besides, the P-values can be calculated following the Equation (6) above. *CDF* represents the cumulative distribution function. *t* means the t-statistic, which could be defined as:

$$t = r \times \sqrt{\frac{n-2}{1-r^2}} \text{ ……..…… (4-7)}$$

Where *r*, *n* are the correlation coefficient from Equation (5) and the number of total samples, respectively. Specifically, the correlation coefficient represents the degree of linear relationship between the two variables, with values ranging from -1 to 1. A value of 1 indicates a perfect positive linear correlation, while a value of -1 indicates a perfect negative linear correlation. P-value, measures the probability of observing a correlation coefficient as extreme as the one obtained by chance, assuming that there is no true correlation between the two variables. The P-value below a certain threshold (e.g., 0.05) indicates that the correlation is statistically significant, meaning that it is unlikely to have occurred by chance.

First of all, we generated the flood risk map, shown in Figure 9, and ranked risks into 5 classes (minimal risk, low risk, moderate risk, high risk, maximal risk) employing the AHP methodology of section. Then, we utilized Pearson correlation analysis as the chosen statistical approach to quantify the relationship between the flood risk map and the flood monitoring result in the Vientiane sub region of Figure 9. As a result, the final correlation coefficients and P-values from 2018 to 2022 are presented in Figure 10. The mean values of correlation coefficients and P-values in five years were assigned to 0.7144 and 0.021, respectively

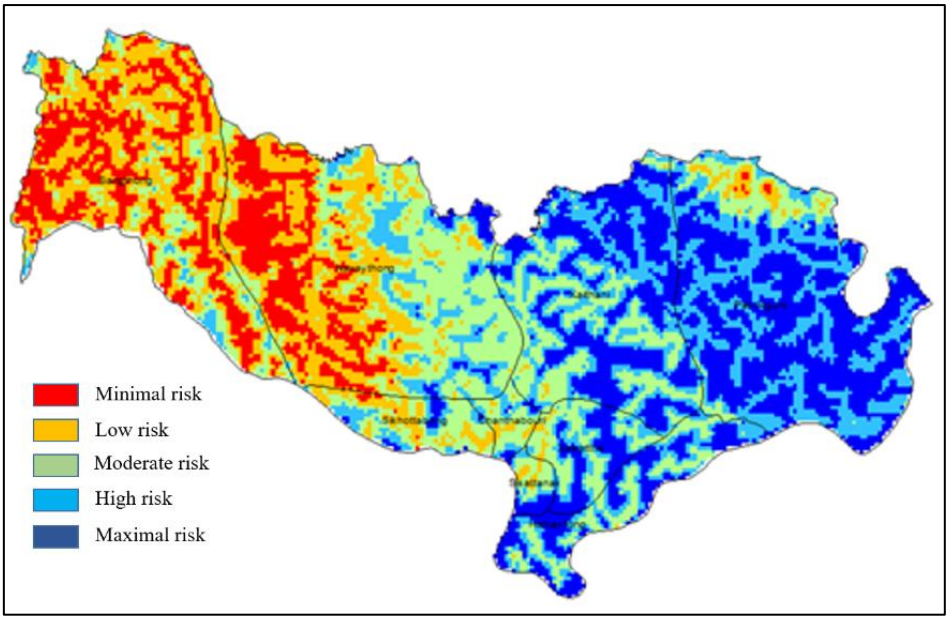

Figure 9: Flood risk map of Vientiane Capital, Laos

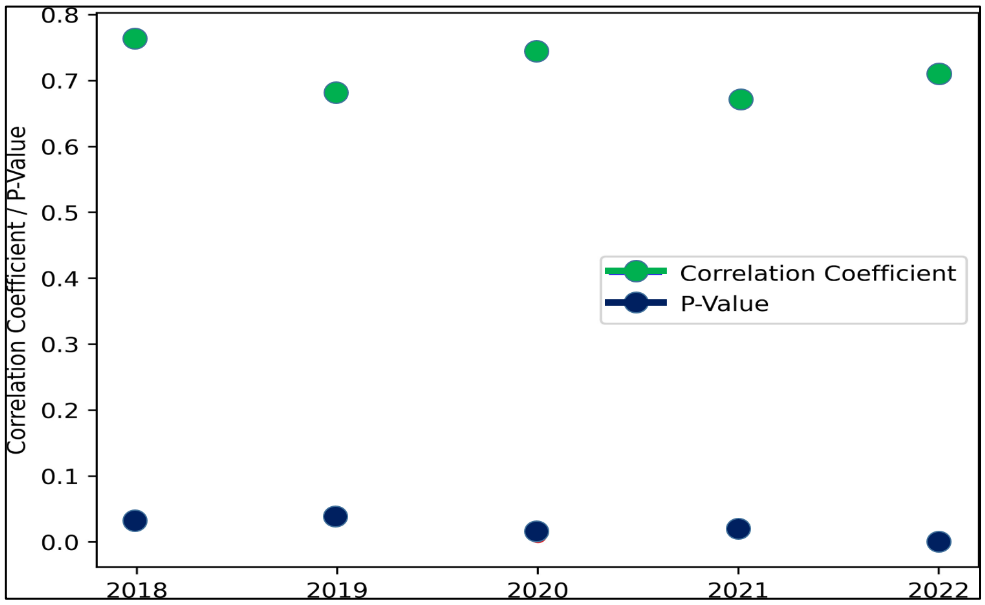

Figure 10: Correlation between flood risk map and flood monitoring map, from 2018 to 2022

IV. DISCUSSION

Additionally, supplementary data such as rainfall records, digital elevation models (DEMs), river networks, and proximity to waterways were integrated into the AHP methodology. This provided a comprehensive understanding of the factors influencing flood occurrences and enabled the creation of a more precise flood vulnerability map. The effectiveness and scientific rigor of the proposed approach were validated using Pearson correlation analysis, which examined the relationship between flood vulnerability and flooding outcomes. Additionally, the research included a comprehensive examination of flood occurrence and its effects within the study area at macroscopic, mesoscopic, and microscopic scales. This methodology demonstrated its efficacy and academic robustness, making it a valuable tool for evaluating and monitoring flood risk in other regions.

A meticulous manual annotation process was employed to generate validation data for a specific area in Vientiane. The comprehensive accuracy evaluation of the identified flood regions clearly demonstrated their exceptional reliability and precision.

V. CONCLUSION

The flood risk level was evaluated using the Analytical Hierarchy Process (AHP) method, incorporating essential data such as rainfall, digital elevation models (DEMs), and river networks. Next, a correlation analysis was performed to compare flood detection results with the flood risk map. Notably, the

proposed methodology demonstrated outstanding efficiency; the methodology achieved an average correlation coefficient of 0.7144 over a five-year period, indicating a substantial level of precision in forecasting flood risk levels. Importantly, the examination was conducted using data collected from various geographic areas, highlighting the strength and versatility of the proposed approach. Furthermore, the Analytical Hierarchy Process (AHP) technique helped precisely identify the factors influencing flood risk, enhancing the understanding of the mechanisms driving flood vulnerability.

REFERENCE

1. Kablan, M. K. A., Dongo, K., & Coulibaly, M. (2017). Assessment of social vulnerability to flood in urban Cote d ˆ ' Ivoire using the MOVE framework. *Water*, *9*(4), 292.
2. Saaty, T. L. (2004). Decision making—the analytic hierarchy and network processes (AHP/ANP). *Journal of systems science and systems engineering*, *13*, 1-35.
3. Das, S. (2018). Geographic information system and AHP-based flood hazard zonation of Vaitarna basin, Maharashtra, India. *Arabian Journal of Geosciences*, *11*(19), 576.
4. Sahani, J., Kumar, P., Debele, S., Spyrou, C., Loupis, M., Aragão, L., ... & Di Sabatino, S. (2019). Hydro-meteorological risk assessment methods and management by nature-based solutions. *Science of the Total Environment*, *696*, 133936.
5. Ghasemlounia, R., & Utlu, M. (2021). Flood prioritization of basins based on geomorphometric properties using principal component analysis, morphometric analysis and Redvan's priority methods: A case study of Harşit River basin. *Journal of Hydrology*, *603*, 127061.
6. Gigović, L., Pamučar, D., Bajić, Z., & Drobnjak, S. (2017). Application of GIS-interval rough AHP methodology for flood hazard mapping in urban areas. *Water*, *9*(6), 360.
7. Lyu, H. M., Sun, W. J., Shen, S. L., & Arulrajah, A. (2018). Flood risk assessment in metro systems of mega-cities using a GIS-based modeling approach. *Science of the Total Environment*, *626*, 1012-1025.
8. Cai, S., Fan, J., & Yang, W. (2021). Flooding risk assessment and analysis based on GIS and the TFN-AHP method: a case study of Chongqing, China. *Atmosphere*, *12*(5), 623.
9. Deng, X., Hu, Y., Deng, Y., & Mahadevan, S. (2014). Supplier selection using AHP methodology extended by D numbers. *Expert Systems with Applications*, *41*(1), 156-167.
10. Fan, G., Zhong, D., Yan, F., & Yue, P. (2016). A hybrid fuzzy evaluation method for curtain grouting efficiency assessment based on an AHP method extended by D numbers. *Expert Systems with Applications*, *44*, 289-303.
11. Yang, J., & Zhao, C. (2019). Survey on K-Means clustering algorithm. *Computer engineering and applications*, *55*(23), 7-14.
12. Xu, H., Ma, C., Lian, J., Xu, K., & Chaima, E. (2018). Urban flooding risk assessment based on an integrated k-means cluster algorithm and improved entropy weight method in the region of Haikou, China. *Journal of hydrology*, *563*, 975-986.
13. Deng, X., & Deng, Y. (2019). D-AHP method with different credibility of information. *Soft Computing*, *23*, 683-691.
14. Giordan, D., Notti, D., Villa, A., Zucca, F., Calò, F., Pepe, A., ... & Allasia, P. (2018). Low cost, multiscale and multi-sensor application for flooded area mapping. *Natural Hazards and Earth System Sciences*, *18*(5), 1493-1516.
15. Sofia, G., Roder, G., Dalla Fontana, G., & Tarolli, P. (2017). Flood dynamics in urbanised landscapes: 100 years of climate and humans' interaction. *Scientific reports*, *7*(1), 40527.
16. Termeh, S. V. R., Kornejady, A., Pourghasemi, H. R., & Keesstra, S. (2018). Flood susceptibility mapping using novel ensembles of adaptive neuro fuzzy inference system and metaheuristic algorithms. *Science of the Total Environment*, *615*, 438-451.
17. Rahmati, O., Zeinivand, H., & Besharat, M. (2016). Flood hazard zoning in Yasooj region, Iran, using GIS and multi-criteria decision analysis. *Geomatics, Natural Hazards and Risk*, *7*(3), 1000-1017.
18. Oeurng, C., Sauvage, S., & Sánchez-Pérez, J. M. (2011). Assessment of hydrology, sediment and particulate organic carbon yield in a large agricultural catchment using the SWAT model. *Journal of Hydrology*, *401*(3-4), 145-153.
19. Choubin, B., Moradi, E., Golshan, M., Adamowski, J., Sajedi-Hosseini, F., & Mosavi, A. (2019). An ensemble prediction of flood susceptibility using multivariate discriminant analysis, classification and regression trees, and support vector machines. *Science of the Total Environment*, *651*, 2087-2096.
20. Tellman, B., Kuhn, C., Max, S. A., & Sullivan, J. (2015, December). Dynamic Flood Vulnerability Mapping with Google Earth Engine. In *AGU Fall Meeting Abstracts* (Vol. 2015, pp. NH51E-1953).
21. Liu, C. C., Shieh, M. C., Ke, M. S., & Wang, K. H. (2018). Flood prevention and emergency response system powered by Google Earth Engine. *Remote sensing*, *10*(8), 1283.
22. Vojtek, M., & Vojteková, J. (2019). Flood susceptibility mapping on a national scale in Slovakia using the analytical hierarchy process. *Water*, *11*(2), 364.
23. Yahaya, S., Ahmad, N., & Abdalla, R. F. (2010). Multicriteria analysis for flood vulnerable areas in Hadejia-Jama'are River basin, Nigeria. *European Journal of Scientific Research*, *42*(1), 71-83.
24. Swain, K. C., Singha, C., & Nayak, L. (2020). Flood susceptibility mapping through the GIS-AHP technique using the cloud. *ISPRS International*

Journal of Geo-Information, *9*(12), 720.
25. Gorelick, N., Hancher, M., Dixon, M., Ilyushchenko, S., Thau, D., & Moore, R. (2017). Google Earth Engine: Planetary-scale geospatial analysis for everyone. *Remote sensing of Environment*, *202*, 18-27.
26. Kumar, L., & Mutanga, O. (2018). Google Earth Engine applications since inception: Usage, trends, and potential. *Remote sensing*, *10*(10), 1509.
27. Padarian, J., Minasny, B., & McBratney, A. B. (2015). Using Google's cloud-based platform for digital soil mapping. *Computers & geosciences*, *83*, 80-88.
28. Xulu, S., Peerbhay, K., Gebreslasie, M., & Ismail, R. (2018). Drought influence on forest plantations in Zululand, South Africa, using MODIS time series and climate data. *Forests*, *9*(9), 528.
29. Vos, K., Splinter, K. D., Harley, M. D., Simmons, J. A., & Turner, I. L. (2019). CoastSat: A Google Earth Engine-enabled Python toolkit to extract shorelines from publicly available satellite imagery. *Environmental Modelling & Software*, *122*, 104528.
30. Fischer, G. (1998). Seeding, evolutionary growth and reseeding: Constructing, capturing and evolving knowledge in domain-oriented design environments. *Automated Software Engineering*, *5*, 447-464.
31. Ermida, S. L., Soares, P., Mantas, V., Göttsche, F. M., & Trigo, I. F. (2020). Google earth engine open-source code for land surface temperature estimation from the landsat series. *Remote Sensing*, *12*(9), 1471.
32. Mutanga, O., & Kumar, L. (2019). Google earth engine applications. *Remote sensing*, *11*(5), 591.
33. Kienberger, S. (2012). Spatial modelling of social and economic vulnerability to floods at the district level in Búzi, Mozambique. *Natural Hazards*, *64*, 2001-2019.
34. Brunner, M. I., Slater, L., Tallaksen, L. M., & Clark, M. (2021). Challenges in modeling and predicting floods and droughts: A review. *Wiley Interdisciplinary Reviews: Water*, *8*(3), e1520.
35. Norallahi, M., & Seyed Kaboli, H. (2021). Urban flood hazard mapping using machine learning models: GARP, RF, MaxEnt and NB. *Natural Hazards*, *106*, 119-137.
36. Jehanzaib, M., Ajmal, M., Achite, M., & Kim, T. W. (2022). Comprehensive review: Advancements in rainfall-runoff modelling for flood mitigation. *Climate*, *10*(10), 147.
37. Hansana, P., Guo, X., Zhang, S., Kang, X., & Li, S. (2023). Flood analysis using multi-scale remote sensing observations in Laos. *Remote Sensing*, *15*(12), 3166.